Abrasive Water Jet Machining Studies on $AlSi_7$+63%SiC Hybrid Composite

Pruthviraju Garikipati and K. Balamurugan

Abstract To improve the properties of Al/Si_7 composite, 63% SiC (maximum solubility) is added as a secondary reinforcement to form Al/Si_7+63%SiC hybrid matrix composite. Al/Si_7+63% SiC composite is fabricated through stir casting process. The fabricated composite is machined by using abrasive water jet machine (AWJM) and an optimum machining condition is evaluated through gray-related response surface method (G-RSM) by using L_{20} orthogonal array. AWJM are governed with independent parameters such as jet pressure (JP), stand-off distance (SOD), and traverse speed (TS). The dependent responses are taken as material removal rate (MRR) and surface roughness (Ra). The effect of each independent parameter and the output responses is evaluated. The optimum machining condition is predicted through ANOVA. The test experiment is conducted to validate the RSM equation, and it found in the acceptable range.

Keywords Al/si_7+63%SiC hybrid composite · Abrasive water jet machine · G-RSM · ANOVA · Optimization

1 Introduction

The advantages of the composite over the conventional materials make a suitable candidate material in mass-market products, like automobiles, aeronautics, etc. [1, 2]. Aluminum composites are prepared using a ceramic mixture, due to its specific strength and excellent stiffness property even at elevated temperature it gain attention in automotive engines components [3, 4]. The addition of 2 wt% of silica will enhance the ductile property of the alloy with the formation of spheroidization in the eutectic solidification [5]. Microscopy analysis of Al-SiC composite surface reveals that the crack initiation starts at SiC particle-rich zone [6]. Also, it is stated that the addition of SiC as a reinforcement material will improve the machinability through the breakup

P. Garikipati · K. Balamurugan (✉)
Department of Mechanical Engineering, VFSTR (Deemed to be University), Guntur, AP 522213, India
e-mail: kbalan2000@gmail.com

A. Arockiarajan et al. (eds.), *Advances in Industrial Automation and Smart Manufacturing*, Lecture Notes in Mechanical Engineering,
https://doi.org/10.1007/978-981-15-4739-3_66

of the particle. Addition of reinforced particles with a homogeneous distribution will lead to a reduction in porosity and improves bonding strength [7]. Fracture mechanics analysis on Al/SiC is the ductile mode of failure. Fracture analysis on Al/SiC is the ductile mode of failure and this occurs due to deformation, crack propagation along with there inforcement particles and through the voids [8]. The machined surface of Al/SiC composite will have plastic deformation surface and the failure occurs at the interfacial de-bonding regions that lead to an early stage of the fracture [9, 10].

Present work will investigate the AWJM performance on $AlSi_7$+63%SiC hybrid composite. The experimental results are optimized using G-RSM. The role of SiC in the hybrid composite is analyzed, and trial experiments are conducted to validate the experimental results.

2 Material Preparation

The preparation of AlSi7% with 63% SiC is done in an induction furnace by mixing the SiC containing zero impurities with $AlSi_7$ alloy. The temperature of the furnace is reduced to 600 °C which cools the liquid alloy for the incorporation of SiC. The secondary reinforcement (SiC) is pre-oxidized at 900 °C for 2 h and reinforcement abrasive grade with size ranging from 15 to 30 micrometers at the constant rate of SiC is added to the semi-solid matrix alloy with specially designed stirrer semi-solid matrix alloy is mixed in the presence of argon gas productive atmosphere production of the metal matrix and composite is carried out. The melt is heated to 750 °C and the temperature is maintained for 5 min with the continuous stirring condition. The composite slurry has been transferred into preheated iron dies that have the wall thickness of 8 mm. Samples of size 25 cm × 25 cm × 1.2 cm is produced after the removal of the feeder head. Addition of more than 63% of SiC in Al7%Si alloys leads to having improper dispersion and hence the maximum solubility of SiC in Al alloy is resisted with 63% of weight ratio.

3 Experimentations and Observations

The machinability of the fabricated hybrid metal matrix composites that find applications in aerospace and automotive industries is examined using AWJM. Garnet is used as abrasive that has the mesh size of 80. The high-pressure jet passes to 0.67 mm diameter WC nozzle where the entire unit is controlled by PLC. The nozzle is kept perpendicular to the cut material. The experimental setup is shown in Fig. 1.

Among various parameters of AWJM, jet pressure (JP), stand-off distance (SOD), and traverse speed (TS) are chosen parameters with three levels [11]. Through central composite design, theoptimum conditions are predicted. The AWJM parameters are listed in Table 1.

Fig. 1 Abrasive water jet machine and the test sample

Table 1 Machining parameters and its levels

S. No.	Machining parameters	Levels			Units
		1	2	3	
1	JP	220	240	260	bar
2	SOD	1	2	3	mm
3	TS	20	30	40	mm/min

4 Results and Discussion

Gray theory-based response surface methodology (G-RSM)

To identify the optimum condition for the multi-level responses for any machining, gray relational analysis (GRA) uses S/N ratio to obtain a feasible solution for producing kerf surfaces with acceptable level of surface properties [12]. RSM is a statistical tool used to get a quadratic equation for GRG. G-RSM technique is used to predict the optimal parameters condition. Table 2 shows the experimental observations of the hybrid composite in AWJM.

Table 2 Machining data: Al/Si_7+63%SiC composite

Test numbers	Machining parameters			Output responses	
	JP	SOD	TS	MRR	Ra
	(bar)	(mm)	(mm/min)	(g/s)	(μm)
1	220	1	20	0.0042	3.047
2	240	2	30	0.0064	3.592
3	260	3	40	0.0090	3.678
4	240	2	40	0.0086	3.622
5	260	3	20	0.0052	3.596
6	240	2	30	0.0065	3.599
7	260	2	30	0.0065	3.908
8	260	1	40	0.0078	4.415
9	240	3	30	0.0072	3.418
10	240	2	30	0.0064	3.613
11	260	1	20	0.0044	4.445
12	220	3	20	0.0048	3.495
13	220	1	40	0.0070	3.097
14	240	2	20	0.0046	3.606
15	220	2	30	0.0060	3.346
16	240	2	30	0.0063	3.511
17	220	3	40	0.0081	3.386
18	240	2	30	0.0064	3.603
19	240	2	30	0.0065	3.599
20	240	1	30	0.0055	3.733

ANOVA for MRR and Ra of fabricate composite are shown in Table 3. Probability value of MRR and Ra is tabulated as zero. The significant effect of the independent parameters could be identified through the least *P*-value. Further, from the *F*-value, it could be stated that the effect of TS is superior to SOD and JP. The interface between JP × TS has found to have the least significant effect over other interfaces. The effect of SOD on output responses is found to be negligible for MRR, whereas the machining parameters of AWJM, i.e., JP and SOD are having a significant effect on Ra. The influence of TS is found to be very low and has no effect. The above observations can be confirmed through the ANOVA table. The interface effect of JP × SOD has a significant effect than other interface parameters on Ra.

Machining effect: MRR

From Fig. 2a, it is observed that at a lower level of SOD and JP, MRR get considerably decreased. At the middle level of JP and SOD, MRR is increased. Increase in SOD, high-pressure jet accelerates the hard abrasive and tends to increase the width of the jet before it impinges the top surface of the composite material. At the high level

Table 3 ANOVA table: MRR and Ra

Source	DF	Adj SS	Adj MS	*F*-value	*P*-value
ANOVA table: MRR					
Model	6	0.000034	0.000006	117.33	0.000
Linear	3	0.000034	0.000011	233.02	0.000
JP	1	0.000001	0.000001	16.53	0.001
SOD	1	0.000003	0.000003	60.95	0.000
TS	1	0.000030	0.000030	621.58	0.000
2-Way interface	3	0.000000	0.000000	1.64	0.229
JP × SOD	1	0.000000	0.000000	0.17	0.691
JP × TS	1	0.000000	0.000000	2.87	0.114
SOD × TS	1	0.000000	0.000000	1.88	0.193
Error	13	0.000001	0.000000	13.28	0.006
Lack-of-fit	8	0.000001	0.000000		
Pure error	5	0.000000	0.000000		
Total	19				
$R^2 = 98.19\%$, Adjacent $R^2 = 97.35\%$					
Source	DF	Adj SS	Adj MS	*F*-value	*P*-value
ANOVA table: Ra					
Model	6	2.16001	0.36000	85.68	0.000
Linear	3	1.48337	0.49446	117.67	0.000
JP	1	1.34799	1.34799	320.80	0.000
SOD	1	0.13537	0.13537	32.22	0.000
TS	1	0.00001	0.00001	0.00	0.964
2-Way interface	3	0.67664	0.22555	53.68	0.000
JP × SOD	1	0.67483	0.67483	160.60	0.000
JP × TS	1	0.00153	0.00153	0.36	0.557
SOD × TS	1	0.00028	0.00028	0.07	0.800
Error	13	0.05463	0.00420	4.24	0.064
Lack-of-fit	8	0.04760	0.00595		
Pure error	5	0.00702	0.00140		
Total	19				
$R^2 = 97.53\%$, Adjacent $R^2 = 96.40\%$					

operating conditions of JP and SOD abrasives will easily erode away the composite surface that significantly increases the MRR. As the hard abrasives hit the surface of the composite since most of the region in the composite is packed with hard SiC particles leads to the excess removal of materials and increases MRR.

In Fig. 2b, increase in JP and TS shows a considerable increase in MRR. It is believed that at high operating condition, the highly accelerated abrasives grains cut composite with bulk removal of SiC material. SOD has high significance compared to JP. From Fig. 2c, the interfaces between SOD and TS are identified to have the least significant effect. However, with an increase in SOD will influence the width of the water beam that leads to getting high MRR. From Fig. 2d, all the experimental

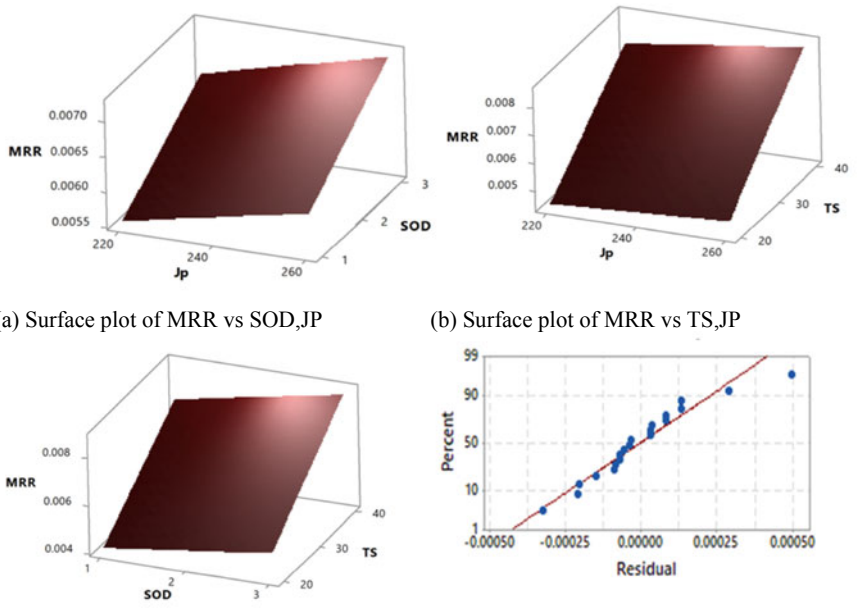

(a) Surface plot of MRR vs SOD,JP

(b) Surface plot of MRR vs TS,JP

(c) Surface plot of MRR vs TS, SOD

(d) Normal Probability of MRR

Fig. 2 Interface plots of the independent parameters on MRR

observations are bound to be in the acceptable level. The optimum machining condition for MRR is identified as with the following conditions: JP = 220 bar, SOD = 1 mm, and TS = 29.2 mm/s.

The predicted equation for MRR is shown in Eq. 1. The residual square of MRR is 98.19% and adjacent of MRR is 97.35% which fits more than 95% of a confidential level.

$$\text{MRR} = 0.00283 - 0.000009\,\text{JP} - 0.000156\,\text{SOD} - 0.00006\text{TS} + 0.000002\,\text{JP} \times \text{SO} + 0.000001\,\text{JP} \times \text{TS} + 0.000011\,\text{SOD} \times \text{TS} \quad (1)$$

Machining effect: Ra

3D surface plot of Ra is displayed at Fig. 3. The interface effect of JP × SOD on Ra is shown in Fig. 3a. The saddle point could not be obtained from the plot, but the optimum surface can be identified through visual inspection. Figure 3b shows the interface effect of JP and TS on Ra. An increase in the levels of JP and TS will increase the surface wear rate and progress to have excess wear track on the cut surface. This action increases Ra value to a greater extent. Figure 3c shows the interface effect of SOD × TS on Ra and the effects produce by SOD on Ra is superior to TS on Ra. It becomes possible to predict the optimum condition under this working condition. To obtain the acceptable level of Ra, AWJM parameters are to be at the levels as JP

of 220 bar, SOD of 1.1 mm, and TS of 21 mm/min. From Fig. 3a–c, it is seen that all considered machining parameters have a major impact on Ra. Figure 3d shows the normal probability plot of the experimental observations. Observations are found to be within the acceptable range.

The equation predicted for Ra is displayed as Eq. 2. From ANOVA table, it is clear that the residual square and adjacent to residual square of Ra is 97.53% and 96.5%, respectively.

$$\begin{aligned} \text{Ra} = &-7.07 + 0.04533\ \text{JP} + 3.387\ \text{SOD} - 0.0153\text{TS} - 0.01452\ \text{JP} \times \text{SOD} \\ &+ 0.000069\ \text{JP} \times \text{TS} - 0.00059\ \text{SOD} \times \text{TS} \end{aligned} \tag{2}$$

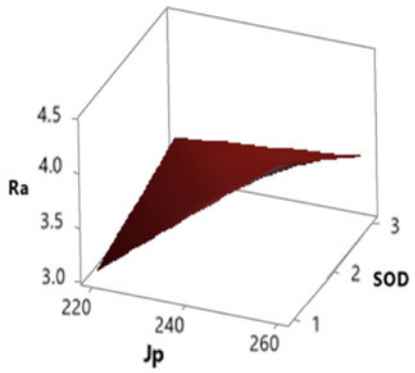

(a)Surface plot of Ra vs SOD,JP

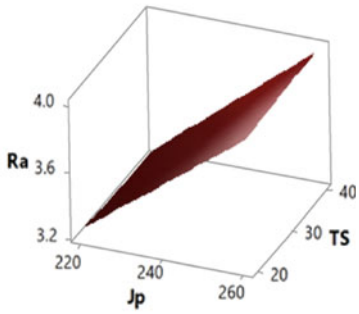

b)Surface plot of Ra vs SOD,JP

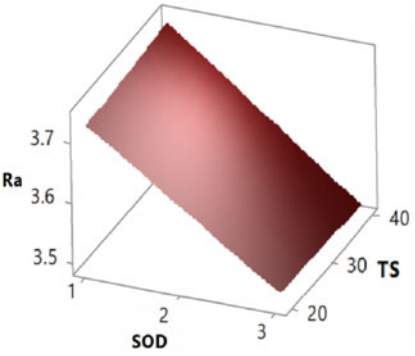

(c) Surface plot of Ra vs SOD,JP

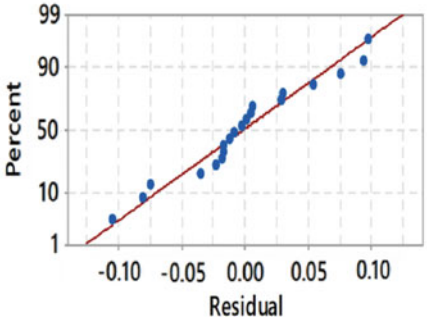

(d) Normal Probability of Ra

Fig. 3 Interface plots of the independent parameters on Ra

5 Experimental Validation

To validate the equations obtained through G-RSM, a trial experiment is performed. The trial machining conditions with the experimental and predicted observations are shown in Table 4. Almost all the predicted observations through the equations are found to be consistent with the experimental observations, and this could be validated through the comparison chart between the experimental and predicted observation and it is shown in Fig. 4.

Table 4 Validation table

Ex. No.	JP	SOD	TS	MRR		Ra	
	(bar)	(mm)	(mm/min)	Experiment	Predicted	Experiment	Predicted
1	245	35	50	0.0125	0.0141	3.392	3.414

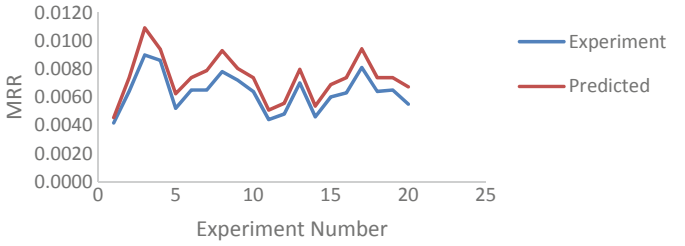

(a) MRR

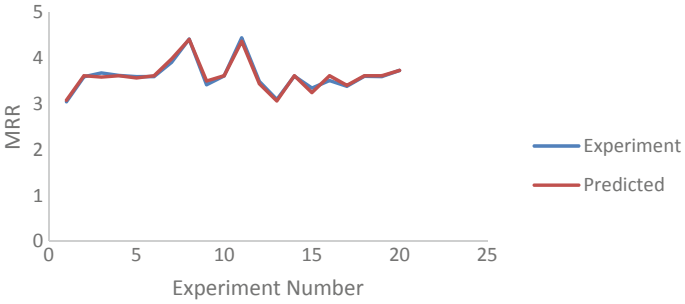

(b) Ra

Fig. 4 Experimental versus predicted observation

6 Conclusions

The parametric investigation on AWJM effects on $AlSi_7$+63%SiC composite is performed and the following conclusion is drawn:

- Jet pressure, stand-off distance, and traverse speed have found to have an important effect over the output responses. The impact of SOD and TS is proved to have greater effect on MRR whereas influence of JP and SOD is higher for Ra.
- Optimized AWJM conditions for MRR is identified as: JP at 20 bar, SOD at 1mmand TS of 29.2 mm/min and to obtain the optimized Ra, the preferable machining condition: JP of 220 bar, SOD of 1.1 mm and TS of 21 mm/s.
- It is observed that the predicted equation best fits the experimental observation and it can be verified by validation table and figure.

References

1. Kaczmar JW, Pietrzak K, Wlosinski W (2000) The production and application of metal matrix composite materials. J Mater Process Technol 106:58–67
2. Valente M, Billi F (2001) Micromechanical modification induced by cyclic thermal stresses on metal matrix composites for automotive applications. Compos: Part B 32:529–533
3. Kelly A, Zweben C (2000) Comprehensive composite materials, vol 3. Elsevier Science Ltd., Oxford
4. Schnabl A, Degischer HP (2003) Thermal cycling creep of a short fiber reinforced aluminium piston alloy. Mater Res Adv Tech 94:743–748
5. Lasagni F, Lasagni A, Holzapfel C, Mucklich F, Degischer HP (2007) Three-dimensional characterization of 'As-Cast' and solution-treated AlSi12(Sr) Alloys by high-resolution FIB tomography. Acta Mater 55:3875–3882
6. Yotte S, Breysse D, Riss J, Ghosh S (2001) Cluster characterization in a metal matrix composite. Mater Charact 46:211–219
7. Lee HS, Yeo JS, Hong SH, Yoon DJ, Na KH (2001) The fabrication process and mechanical properties of SiCp/Al-Si metal matrix composites for automobile air-conditioner compression pistons. J Mater Process Technol 113:202–208
8. Pandey AB, Majumdar BS, Miracle DB (2000) Deformation and fracture of a particle-reinforced aluminum alloy composite: part I. Experiments. Metall Mater Trans A 31:921–936
9. Badini C, La Vecciha M, Giurcanu A, Wenhui J (1997) Damage of 6061/SiCw composite by thermal cycling. J Mater Sci 32:921–930
10. Manikandan N, Binoj JS, Varaprasad KC, Sabari SS, Raju R (2019) Investigations on wire spark Erosion machining of aluminum-based metal matrix composites. Lecture Notes in Mechanical Engineering, Advances in Manufacturing Technology, Springer, Singapore, pp 361–369
11. Balamurugan K, Uthayakumar M, Sankar S, Hareesh US, Warrier KGK (2018) J Aust Ceramic Soc 54:205. https://doi.org/10.1007/s41779-017-0142-7
12. Ghosh D, Doloi B, Das PK (2015) Parametric analysis and optimization on abrasive water jet cutting of silicon nitride ceramics. J Precis Technol 5:294–311